Amphiphilic Model Conetworks Based on Cross-Linked Star Copolymers of Benzyl Methacrylate and 2-(Dimethylamino)ethyl Methacrylate: Synthesis, Characterization, and DNA Adsorption Studies

Demetra S. Achilleos, Theoni K. Georgiou, and Costas S. Patrickios*

Department of Chemistry, University of Cyprus, P. O. Box 20537, 1678 Nicosia, Cyprus

Received July 18, 2006; Revised Manuscript Received September 19, 2006

Six amphiphilic model conetworks of a new structure, that of cross-linked "in−out" star copolymers, were synthesized by the group transfer polymerization (GTP) of the hydrophobic monomer benzyl methacrylate (BzMA) and the ionizable hydrophilic monomer 2-(dimethylamino)ethyl methacrylate (DMAEMA) in a one-pot preparation. The synthesis took place in tetrahydrofuran (THF) using tetrabutylammonium bibenzoate (TBABB) as the catalyst, 1-methoxy-1-(trimethylsiloxy)-2-methyl-propene (MTS) as the initiator, and ethylene glycol dimethacrylate (EGDMA) as the cross-linker. Three heteroarm star-, two star block-, one statistical copolymer star-, and one homopolymer star-based networks were prepared. The synthesis of these star-based networks involved four to six steps, including the preparation of the linear (co)polymers, the "arm-first" and the "in−out" star copolymers, and finally the network. The precursors and the extractables were characterized using gel permeation chromatography (GPC) and proton nuclear magnetic resonance (^{1}H NMR) spectroscopy. The degrees of swelling (DSs) of all the networks were measured in THF, while the aqueous DSs were measured as a function of pH. The DSs at low pH were higher than those at neutral or high pH because of the protonation of the DMAEMA units and were found to be dependent on the structure of the network. The DSs in THF were higher than those in neutral water and were independent of the structure. Finally, DNA adsorption studies onto the networks indicated that the DNA binding was governed by electrostatics.

Introduction

Amphiphilic polymer conetworks[1,2] are modern materials with unique properties and an increasing number of applications. The amphiphilic nature of these materials enables the swelling in both aqueous and hydrocarbon environments and the adsorption of both polar and nonpolar solutes. Moreover, the arrangement of the conetwork hydrophilic and hydrophobic units in separate and sufficiently long segments leads to microphase separation,[3,4] analogous to the micellization of linear block copolymers. Applications of amphiphilic conetworks include uses as matrices for drug delivery[5−8] and for the preparation of inorganic nanoparticles,[9] supports for enzymes,[10] scaffolds for tissue engineering[11,12] and for implantation,[13] and are the materials from which soft contact lenses[14] are prepared where softness, mechanical strength,[15] and oxygen permeability[15,16] need to be combined.

When the amphiphilic conetworks have a controlled structure, bearing chains of well-defined molecular weight and composition, these conetworks are called model.[17] The synthesis of model amphiphilic conetworks (MACs) requires the use of "living"/controlled polymerization techniques,[18] which produce homogeneous polymer chains. The difficulties in employing those techniques in nonspecialized laboratories preclude the wide production of MACs, restricting it to less perfect amphiphilic conetworks in which either part of or the whole conetwork is prepared by free-radical polymerization.

Over the past 6 years, our research team has prepared several series of polymethacrylate MACs[19] using group transfer polymerization (GTP),[20−24] a "quasi-living" polymerization technique whose active species is an enolate anion. Most of our syntheses involved the use of a bifunctional GTP initiator and the sequential polymerization of two monomers (one hydrophilic and the other hydrophobic) and the cross-linker to obtain MACs based on end-linked ABA triblock copolymers.[25−28] This procedure is accomplished in only three polymerization/addition steps and results in the preparation of the simplest MAC structure named "regular" MAC. In a more recent approach, we developed a procedure for the synthesis of MACs employing a monofunctional initiator but requiring up to six polymerization/addition steps.[29−32] The resulting structure consists of interconnected amphiphilic star copolymers and has been named "cross-linked star" MAC (CLS-MAC).

Despite the novelty of the CLS structure, to date we have prepared only one example of CLS-MACs[30] in which the simplest methacrylate monomer, methyl methacrylate (MMA), was used for the hydrophobic units. The objective of the present work was to expand on our previous work on CLS-MACs by exploring the introduction of a different and less common hydrophobic monomer, benzyl methacrylate (BzMA). BzMA is more hydrophobic and bulkier than MMA. Moreover, the BzMA units can be readily hydrogenolyzed after the polymerization to hydrophilic methacrylic acid (MAA) units.[33,34] In this investigation, BzMA was combined with the hydrophilic monomer 2-(dimethylamino)ethyl methacrylate (DMAEMA) to prepare several CLS-MACs based on different isomeric amphiphilic star structures. The resulting CLS-MACs were studied in terms of their swelling in aqueous and organic media and were characterized in terms of their ability to adsorb DNA. DNA binding to synthetic cationic star polymers is a field of major

* Corresponding author. E-mail: costasp@ucy.ac.cy.

10.1021/bm060699m CCC: $33.50
Published on Web 11/07/2006

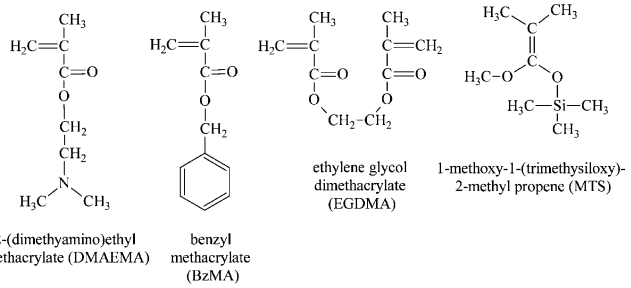

Figure 1. Chemical structures and names of the main reagents used for the network synthesis.

interest in our laboratories and is exploited for DNA delivery into cells.[35−37]

Experimental Section

Network Synthesis. *Materials.* The monomers, benzyl methacrylate (BzMA, hydrophobic, 96%) and 2-(dimethylamino)ethyl methacrylate (DMAEMA, hydrophilic and ionizable, 98%), the cross-linker, ethylene glycol dimethacrylate (EGDMA, 98%), the initiator, 1-methoxy-1-(trimethylsiloxy)-2-methyl propene (MTS, 95%), tetrabutylammonium hydroxide (40% in water), benzoic acid (99.5%), calcium hydride (CaH_2, 90−95%), 2,2-diphenyl-1-picrylhydrazyl hydrate (DPPH, free-radical inhibitor, 95%), deoxyribonucleic acid (DNA) from herring's sperm, basic alumina, and potassium metal (98%) were all purchased from Aldrich, Germany. Figure 1 shows the chemical structures and names of the monomers, the cross-linker, and the initiator. Sodium metal was purchased from Fluka, Germany. Tetrahydrofuran (THF, 99.8%) was purchased from Labscan, Ireland and was used both as the polymerization solvent (reagent grade) and as the mobile phase in chromatography (HPLC grade).

Methods. The methods used in this investigation were similar to those employed for typical GTP syntheses. The polymerization solvent, THF, was dried by refluxing it over a potassium/sodium alloy for 3 days prior to use. The monomers and the cross-linker were passed twice through basic alumina columns to remove inhibitors and protic impurities. They were subsequently stirred over CaH_2 in the presence of the DPPH free-radical inhibitor and were stored at 5 °C. The monomers and the cross-linker were freshly distilled under vacuum and kept under a dry nitrogen atmosphere until use. The initiator was distilled once prior to the polymerization. The dried catalyst powder, which was in-house synthesized by the method of Dicker et al.,[22] was stored in a round-bottom flask under vacuum until use. All glassware was dried overnight at 120 °C and assembled hot under dynamic vacuum prior to use.

Polymerizations. The network preparation followed the synthetic procedure established for the synthesis of cross-linked star polymer networks.[29−32] The reactions were carried out in 250 mL round-bottom flasks at room temperature. The polymerization exotherm was monitored by a digital thermometer to follow the progress of the reaction.

The polymerization procedure for the synthesis of one of the cross-linked star block copolymers, network 2, with both the primary (dangling chains) and secondary (elastic chains) arms comprising linear diblock copolymers with 7.5 BzMA and 22.5 DMAEMA units is detailed below and is illustrated schematically in Figure 2. Freshly distilled THF (84 mL), MTS initiator (0.5 mL, 0.43 g, 2.46 mmol), and BzMA (3.2 mL, 3.3 g, 0.019 mol) were syringed in this order to a 250 mL round-bottom flask fitted with a rubber septum, kept under a dry nitrogen inert atmosphere and containing a small amount (∼10 mg, 20 μmol) of TBABB catalyst. The polymerization exotherm (29.5−33.4 °C) abated within 5 min, samples were extracted, and DMAEMA (9.3 mL, 8.7 g, 0.055 mol) was added slowly giving an exotherm (31.8−38.6 °C). After sampling, EGDMA (1.9 mL, 2.0 g, 0.010 mol) was added which produced an exotherm (34.7−36.9 °C) to give "arm-first" star copolymers. Samples were withdrawn again before BzMA (3.2 mL, 3.3 g, 0.019 mol) was added giving an exotherm from 34.6 to 39.4 °C. At this stage, "in−out" star copolymers comprising linear diblock copolymer primary arms and linear homopolymer secondary arms were produced. Next, after sampling again, DMAEMA (9.3 mL, 8.7 g, 0.055 mol) was added with the temperature increasing from 37.3 to 39.4 °C. Samples were withdrawn for the last time before the final step, the addition of EGDMA (1.9 mL, 2.0 g, 0.010 mol), which promoted gelation within seconds.

Characterization of the Network Precursors. *Gel Permeation Chromatography.* The molecular weights (MWs) and the molecular weight distributions (MWDs) of the linear, the "arm-first" star, and the "in−out" star precursors to the CLS-MACs were determined by gel permeation chromatography (GPC) using a single high MW range Polymer Laboratories PL-Mixed "D" column. The mobile phase was THF, delivered at a flow rate of 1 mL min^{-1} using a Polymer Laboratories PL-LC1120 isocratic pump. The refractive index signal was measured using an ERC-7515A refractive index detector also supplied by Polymer Laboratories. The calibration curve was based on eight narrow MW (630, 2600, 4250, 1300, 22 650, 50 000, 128 000, and 260 000 g mol^{-1}) linear polyMMA standards which provided good estimation for the MWs of the linear polymers but only rough estimations for the MWs of the star polymers.

^{1}H NMR Spectroscopy. The compositions of the precursors to and the extractables from the CLS-MACs were determined by proton nuclear magnetic resonance (^{1}H NMR) spectroscopy using a 300 MHz Avance Bruker NMR spectrometer equipped with an Ultrashield magnet. The solvent was $CDCl_3$ containing traces of tetramethylsilane (TMS), which was used as an internal reference.

Characterization of the Networks. *Determination of the Sol Fraction.* The prepared CLS-MACs were taken out of the polymerization flasks and washed in 200 mL of THF for 1 week to remove the sol fraction. Next, the THF solution was recovered by filtration. The extraction procedure was repeated once more after 1 week, and the solvent from the combined extracts was evaporated using a rotary evaporator. The recovered polymer was further dried for 24 h in a vacuum oven at room temperature. The sol fraction was calculated as the ratio of the dried mass of the extracted polymer divided by the theoretical mass of the polymer in the gel. The latter was calculated from the polymerization stoichiometry as the sum of the masses of the monomers, the cross-linker, and the initiator. The dried extractables were subsequently characterized in terms of their MW and composition by GPC and ^{1}H NMR spectroscopy, respectively.

Characterization of the Degree of Swelling. The washed CLS-MACs were cut into small cubes with edge dimensions of ∼10 mm. The mass of the THF-swollen cubes was measured gravimetrically before placing all samples in a vacuum oven for drying for 72 h at room temperature. The dry gel mass was determined, followed by the transfer of the gels in organic solvent (THF) or in water. One sample from each network was allowed to equilibrate in THF, and 12 other samples were allowed to equilibrate in acidic, neutral, and alkaline Milli-Q (deionized) water for 2 weeks. Nine from the 12 samples were acidified by the addition of a calculated volume of a 0.5 M HCl standard solution, such that degrees of ionization between 12% and 100% were achieved. The calculation was based on the measured dry mass of each sample, from which the number of equivalents of DMAEMA units was estimated (granting that all DMAEMA units were not ionized before the addition of HCl). The pH of these nine samples covered the range between 2 and 7. One sample remained neutral (no acid or base was added) and had a pH of 8−9. Two samples became alkaline by the addition of small volumes of a 0.5 M NaOH standard solution. The samples were allowed to equilibrate for 3 weeks. The degrees of swelling (DSs) were calculated as the ratio of the wet network mass divided by the dry network mass. All DSs were determined five times, and the averages of the measurements are presented along with their 95% confidence intervals.

Calculation of Degree of Ionization and the pK. The degree of ionization (DI) of each sample was calculated as the number of HCl

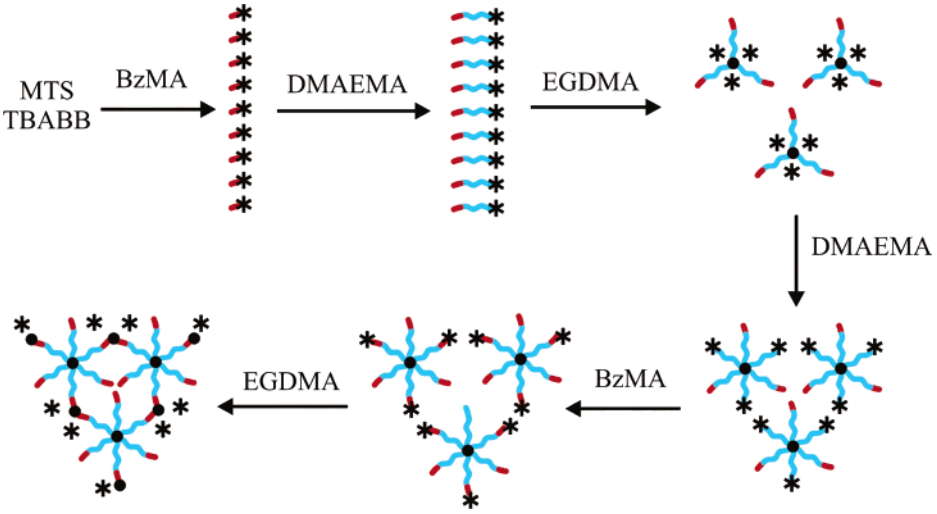

Figure 2. Schematic representation of the synthetic procedure followed for the preparation of the block copolymer-based network 2: ($BzMA_{7.5}$-*b*-$DMAEMA_{22.5}$)-*star*-($DMAEMA_{22.5}$-*b*-$BzMA_{7.5}$)-*network*. The number of arms is not 3/6, as indicated in the figure, but much higher, 30/60. The dark red and light blue colors indicate BzMA and DMAEMA segments, respectively, while the asterisks denote active polymerization sites.

equivalents added divided by the number of DMAEMA unit equivalents present in the sample. The hydrogen ion titration curves were obtained by plotting the calculated DI against the measured solution pH. The effective p*K* of the DMAEMA units of each network was estimated from the hydrogen ion titration as the pH (of the supernatant solution) at 50% ionization.

DNA Adsorption Studies. The synthesized CLS-MACs were used for herring's sperm DNA adsorption studies. First, DNA solutions that span a range of concentrations (1×10^{-7} to 1×10^{-4} g mL^{-1}) were prepared and their absorbance was measured at 260 nm using a Lambda 10 Perkin-Elmer UV−vis spectrometer. A calibration curve [$A = f(C)$] was subsequently constructed. Afterward, choosing one of the more concentrated DNA solutions, the one with a concentration of 4×10^{-5} g mL^{-1}, that presented an absorbance value close to 1, the absorbance was measured as a function of the pH and a calibration curve with respect to the pH [$A = f(pH)$] was constructed. The pH values were adjusted by the addition of the appropriate volume (in number of drops) of 0.5 M HCl and NaOH solution into the DNA solution, taking into account the protonation of the DMAEMA units, to achieve acidic and alkaline pH values, respectively. Next, three or four THF-swollen cubic samples of size of ~10 mm from each network were placed in a vacuum oven and dried at room temperature for 48 h, and they were finally weighed. A volume of 6 mL of the dilute acidic or alkaline solution of DNA was transferred to each vial. Given that DNA precipitates at pH ≤ 4, no solutions were prepared in this range of pH. The samples were allowed to equilibrate for 3 weeks, and the absorbance of the supernatant solutions was measured at 260 nm using the UV−vis spectrometer. The DNA concentration in the supernatant was calculated using the relevant calibration curve. The amount of adsorbed DNA was calculated from the amount initially added and its final concentration in the supernatant. The percentage of adsorption was calculated as the ratio of the amount of the adsorbed DNA divided by the amount of DNA initially loaded. Finally, the pH of the supernatant and the DS of each network were measured.

Results and Discussion

Synthesis and Structure of CLS-MACs. The synthetic sequences used for the preparation of the networks are summarized in Figure 3. The GTP synthesis comprised a successful multi- (4-, 5-, or 6-) step sequential addition in a one-pot preparation. The linear active (co)polymers produced upon the addition of methacrylate monomer(s) to a solution containing the monofunctional GTP initiator and the GTP catalyst were converted to "arm-first" star polymers with active cores upon the addition of the dimethacrylate cross-linker. These "arm-first" star polymers were further grown from the core outward, upon the addition of more monomer(s) to yield the "in−out" star polymers. Finally, the dimethacrylate cross-linker was added a second time to interconnect these stars to a network.

In particular, network 1, the DMAEMA homopolymer cross-linked star network, was prepared by the DMAEMA/cross-linker/DMAEMA/cross-linker sequential additions. The preparation of cross-linked star block copolymers, networks 2 and 3, required the sequential addition of two different monomers before the two EGDMA additions, while the synthesis of the cross-linked statistical copolymer star, network 4, required the simultaneous addition of the two monomers before the cross-linker additions. The cross-linked heteroarm star, network 5, was prepared by the BzMA/cross-linker/DMAEMA/cross-linker sequential additions. The preparation of network 6 required the sequential addition of the two monomers before the first EGDMA addition and afterward the addition of DMAEMA monomer, while network 7 required the simultaneous addition of the two monomers before the first addition of the cross-linker and the last addition of the DMAEMA monomer.

Figure 4 shows all network structures based on cross-linked stars synthesized in this study. In this figure, the DMAEMA units are illustrated in light blue and the BzMA units in dark red, as in Figure 2. Network 1 is the homopolymer. The network structures on the top right, networks 2 and 3, are the two cross-linked star block copolymers whose arms are diblock copolymers. Network 4 is based on cross-linked statistical star copolymers. Network 5 is a heteroarm star-based network whose primary and secondary arms are different types of homopolymers. Networks 6 and 7 are also cross-linked heteroarm star copolymers whose primary arms are diblock copolymers and statistical copolymers, respectively, while the secondary arms are DMAEMA homopolymers for both networks.

Molecular Weights of CLS-MACs. Figure 5 shows the GPC chromatograms of the extractables from and the five precursors to network 2, the cross-linked star block copolymer network ($BzMA_{7.5}$-*b*-$DMAEMA_{22.5}$)-*star*-($DMAEMA_{22.5}$-*b*-$BzMA_{7.5}$)-*network*. The MWDs of the linear BzMA homopolymer ($B_{7.5}$) and the linear BzMA-DMAEMA diblock copolymer ($B_{7.5}$-*b*-$D_{22.5}$) were narrow and unimodal, as expected. The MWD of

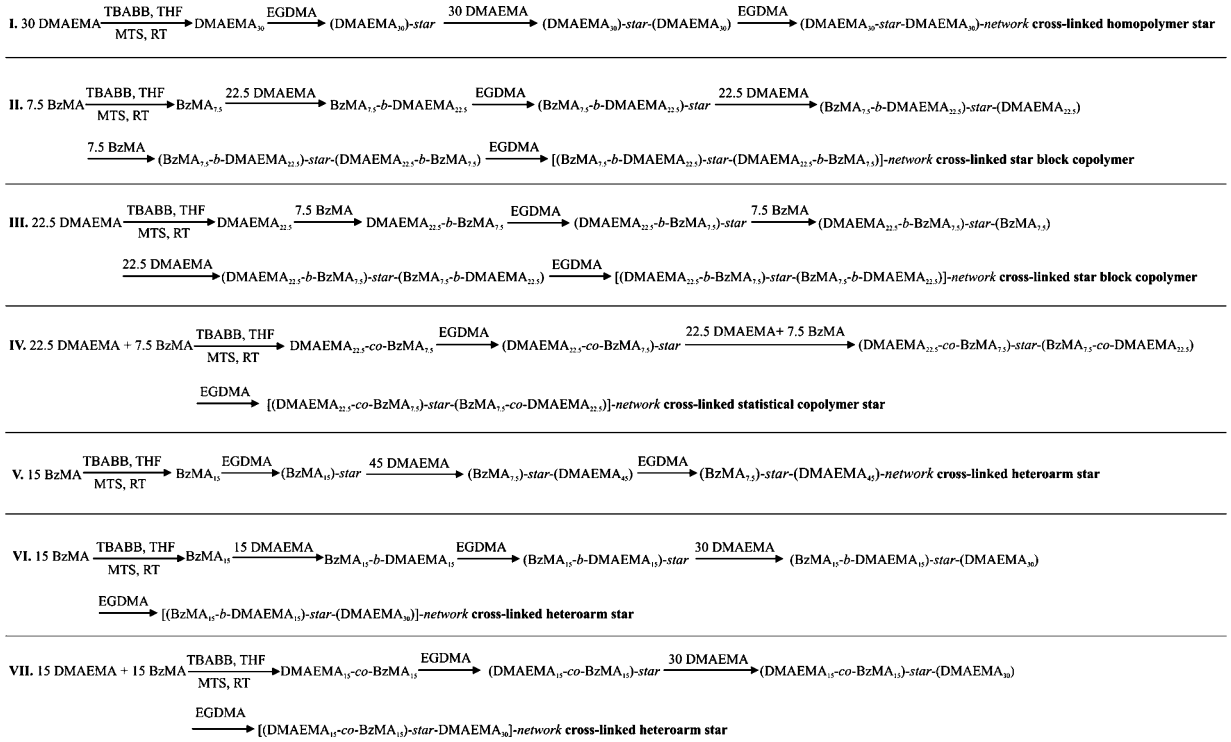

Figure 3. Synthetic sequences employed for the preparation of the various cross-linked star network architectures of this study.

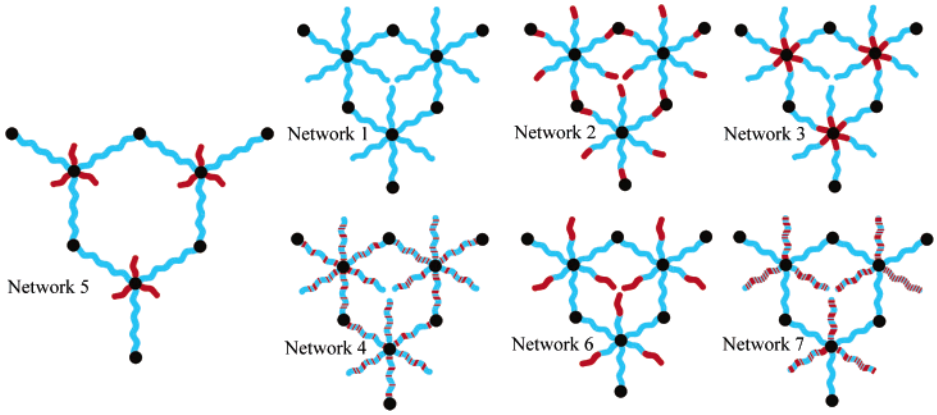

Figure 4. Schematic representation of the architectures of the model networks of this study. The DMAEMA units are depicted light blue, while the BzMA units are colored dark red.

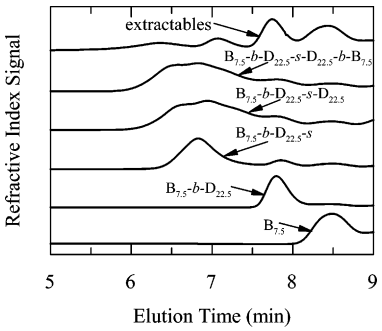

Figure 5. Gel permeation chromatograms of the five precursors to network 2: ($BzMA_{7.5}$-*b*-$DMAEMA_{22.5}$)-*star*-($DMAEMA_{22.5}$-*b*-$BzMA_{7.5}$)-*network*. In the curve labeling, D, B, and *s* are (further) abbreviations for DMAEMA, BzMA, and star, respectively, while the polymer nomenclature follows that introduced in Figure 3.

the "arm-first" star ($B_{7.5}$-*b*-$D_{22.5}$-*s*) was bimodal, containing unattached linear chains in addition to the star. These chains originated from accidental deactivation during synthesis and from steric hindrance, and they consequently could not grow upon further addition of monomer. Similar were the chromatograms of the "in−out" stars, ($B_{7.5}$-*b*-$D_{22.5}$)-*star*-($D_{22.5}$) and ($B_{7.5}$-*b*-$D_{22.5}$)-*star*-($D_{22.5}$-*b*-$B_{7.5}$), which were multimodal with a relatively narrow MWD of the main peak corresponding to the "in−out" star. The MW of the main peak increased from the initial homopolymer to the final "in−out" star precursor, as expected, indicating the growth of the structure as a whole. Similar results were obtained for the precursors to all networks synthesized.

Table 1 shows all the cross-linked star polymers prepared in this study and their GPC characterization data. These include the apparent number-average MWs, M_n's, the polydispersity indices (PDIs, M_w/M_n's), and the peak MWs, M_p's. The M_n's of all linear polymers were almost equal to or slightly higher than the theoretical MWs due to partial initiator deactivation, while their PDIs were low ($\leq$1.25). For the "arm-first" star polymers, the PDIs shown were relatively low ($\leq$1.45) with one exception, network 3, where the peaks of the star and the unattached linear chains were included in the calculation due to their overlap. Similar to the "arm-first" star polymers,

Table 1. GPC and ^{1}H NMR Characterization of the Cross-Linked Star Network Precursors

			GPC results			% mol composition in BzMA	
net no.	theoretical structure[a]	theoretical MW	M_n	M_p	M_w/M_n	theoret	^{1}H NMR
1	D_{30}	4800	4800	5300	1.06		
	D_{30}-*s*	*	25500	30400	1.17		
	D_{30}-*s*-D_{30}	*	26800	35500	1.33		
2	$B_{7.5}$	1400	2100	2200	1.08		
	$B_{7.5}$-*b*-$D_{22.5}$	5000	7000	7500	1.05	25	24
	$B_{7.5}$-*b*-$D_{22.5}$-*s*	*	39600	43900	1.16	25	24
	$B_{7.5}$-*b*-$D_{22.5}$-*s*-$D_{22.5}$	*	36500	62100	1.38	14	14
	$B_{7.5}$-*b*-$D_{22.5}$-*s*-$D_{22.5}$-*b*-$B_{7.5}$	*	44100	76800	1.41	25	24
3	$D_{22.5}$	3600	3500	3900	1.06		
	$D_{22.5}$-*b*-$B_{7.5}$	5000	4700	5200	1.05	25	22
	$D_{22.5}$-*b*-$B_{7.5}$-*s*	*	8100	22600	2.07	25	20
	$D_{22.5}$-*b*-$B_{7.5}$-*s*-$B_{7.5}$	*	36700	45300	1.16	40	32
	$D_{22.5}$-*b*-$B_{7.5}$-*s*-$B_{7.5}$-*b*-$D_{22.5}$	*	47300	61400	1.20	25	17
4	$D_{22.5}$-*co*-$B_{7.5}$	5000	4900	5300	1.07	25	25
	$D_{22.5}$-*co*-$B_{7.5}$-*s*	*	28000	34400	1.16	25	25
	$D_{22.5}$-*co*-$B_{7.5}$-*s*-$B_{7.5}$-*co*-$D_{22.5}$	*	33000	45300	1.27	25	23
5	B_{15}	2800	3000	3500	1.09		
	B_{15}-*s*	*	48300	63300	1.45		
	B_{15}-*s*-D_{45}	*	92600	140100	1.56	25	19
6	B_{15}	2800	2800	3300	1.10		
	B_{15}-*b*-D_{15}	5000	4800	7300	1.25	50	46
	B_{15}-*b*-D_{15}-*s*	*	60100	69400	1.14	50	46
	B_{15}-*b*-D_{15}-*s*-D_{30}	*	88500	109700	1.29	25	24
7	B_{15}-*co*-D_{15}	5102	5500	6000	1.07	50	48
	B_{15}-*co*-D_{15}-*s*	*	40400	46700	1.16	50	49
	B_{15}-*co*-D_{15}-*s*-D_{30}	*	34000	69100	1.37	25	24

[a] D, B, and *s* are (further) abbreviations for DMAEMA, BzMA, and *star*, respectively.

Table 2. Mass Percentage, Molecular Weights, and Compositions of the Sol Fractions Extracted from the Cross-Linked Star Networks, as Measured by Gravimetry, GPC, and ^{1}H NMR

				GPC on extractables			% mol BzMA	by ^{1}H NMR	
net no.	theoretical chemical stucture[a]	extractables w/w %	M_p	M_n	M_w/M_n	theor of precursor	precursor	extract
1	D_{30}-*s*-D_{30}	11.2	5670	5320	1.02	0	0	0
2	$B_{7.5}$-*b*-$D_{22.5}$-*s*-$D_{22.5}$-*b*-$B_{7.5}$	13.4	7970	7590	1.08	25	ND[b]	40
3	$D_{22.5}$-*b*-$B_{7.5}$-*s*-$B_{7.5}$-*b*-$D_{22.5}$	19.2	5500	5140	1.08	25	17	18
4	$D_{22.5}$-*co*-$B_{7.5}$-*s*-$B_{7.5}$-*co*-$D_{22.5}$	12.8	5330	4690	1.08	25	23	26
5	B_{15}-*s*-D_{45}	25.0	3350	2890	1.10	25	19	34
6	B_{15}-*b*-D_{15}-*s*-D_{30}	16.6	3240	3050	1.23	25	24	32
7	B_{15}-*co*-D_{15}-*s*-D_{30}	14.3	5670	4790	1.12	25	24	54

[a] D, B, and *s* are (further) abbreviations for DMAEMA, BzMA, and *star*, respectively. [b] ND: not determined.

relatively low PDIs ($\leq$1.56) were obtained for the "in−out" stars. Their M_n's were higher than those of the respective "arm-first" stars, as expected, with two exceptions where there was peak overlap. The corresponding M_p's are also provided and exhibited the same trend (increasing), suggesting that the whole distribution grew.

The composition of each network precursor (sampled at every step of the synthetic procedure) was determined from the ^{1}H NMR spectra (Table 1), by ratioing the signal from the two aromatic protons at 4.8 ppm in BzMA to the six protons in the two azamethyl groups at 2.3 ppm in DMAEMA. The percentages of BzMA determined by ^{1}H NMR were found to be close to the theoretically calculated percentages of BzMA. This confirmed that the networks had the desired composition.

Percentage, MW, and Composition of the Sol Fraction of the Networks. Table 2 shows the mass percentage, M_p's, M_n's, and PDIs of the largest peak, and finally the composition of the extractables from each network as measured by gravimetry, GPC, and ^{1}H NMR. With the exceptions of network 3, ($D_{22.5}$-*b*-$B_{7.5}$)-*star*-($B_{7.5}$-*b*-$D_{22.5}$)-*network*, and network 5, (B_{15})-*star*-(D_{45})-*network*, that contained 19% and 25% extractables, respectively, all the other networks exhibited relatively low sol fractions, lower than 17%. The low values of these sol fractions support previous findings[29−32] where a 4:1 molar ratio of the EGDMA cross-linker to the initiator was determined as the optimal ratio for sufficiently high conversion to star polymer during "arm-first" star polymer synthesis. Similar results were also obtained from studies on both the "living" anionic and

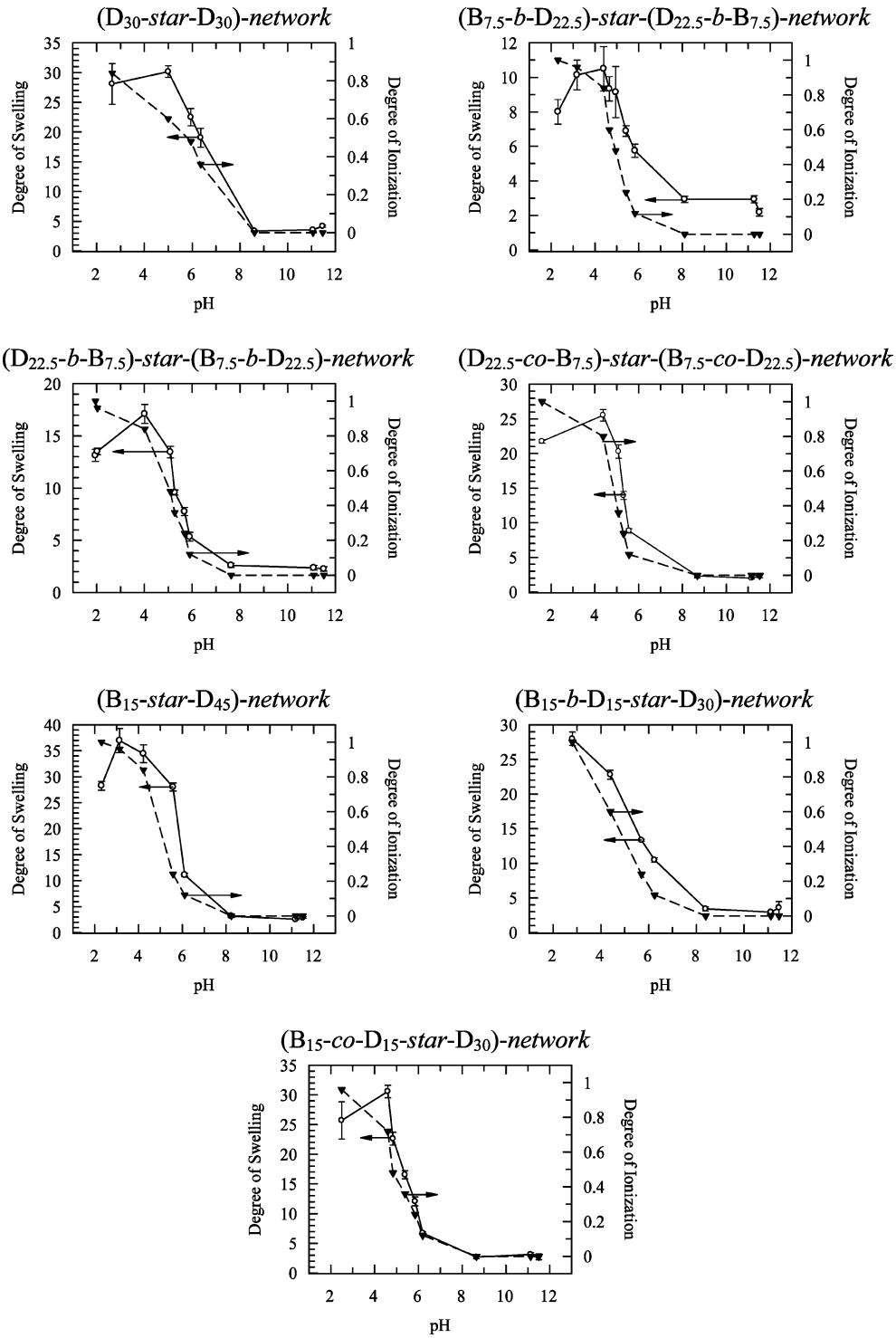

Figure 6. pH dependence of the aqueous degrees of swelling and the degrees of ionization of the cross-linked star networks.

"living" cationic "arm-first" star polymer synthesis[38,39] in which high star polymer yields (>85%) were obtained. These low amounts of extractables measured directly indicate satisfactory control over the network structure during synthesis. In addition to their mass percentage, the relative M_p's, M_n's, and PDIs of the highest peak of the GPC chromatogram and the composition of the extractables are also shown in this table. From these results, the step where the highest deactivation occurred during synthesis can be inferred. For all the networks, the main component of the extractables were the linear precursors that were not attached to the star. The composition of the extractables in most cases was found to be rich in the units of the monomer of the first addition, confirming the previous conclusion that deactivation took place during the early stages of the synthesis. The low values of the M_p's also correspond to linear polymers. The cross-linked heteroarm star copolymer network 5 was the least perfect network, as manifested by the high percentage of extractables already mentioned. Note that network 5 was the only network whose dangling chains comprised linear BzMA homopolymer.

Degrees of Swelling of the Networks. The experimentally measured DSs and DIs of all the networks are plotted against the pH of the supernatant solution in Figure 6. The figure shows that the pH was a factor that profoundly affected the DSs of all

Table 3. Effective p*K*'s of DMAEMA Units of the Cross-Linked Star Networks

net no.	theoretical chemical structure	effective pK
1	($DMAEMA_{30}$-*star*-$DMAEMA_{30}$)-*network*	5.5
2	[($BzMA_{7.5}$-*b*-$DMAEMA_{22.5}$)-*star*-($DMAEMA_{22.5}$-*b*-$BzMA_{7.5}$)]-*network*	5.0
3	[($DMAEMA_{22.5}$-*b*-$BzMA_{7.5}$)-*star*-($BzMA_{7.5}$-*b*-$DMAEMA_{22.5}$)]-*network*	5.0
4	[($DMAEMA_{22.5}$-*co*-$BzMA_{7.5}$)-*star*-($BzMA_{7.5}$-*co*-$DMAEMA_{22.5}$)]-*network*	4.8
5	($BzMA_{15}$-*star*-$DMAEMA_{45}$)-*network*	5.0
6	[($BzMA_{15}$-*b*-$DMAEMA_{15}$)-*star*-($DMAEMA_{30}$)]-*network*	5.0
7	[($BzMA_{15}$-*co*-$DMAEMA_{15}$)-*star*-($DMAEMA_{30}$)]-*network*	5.0

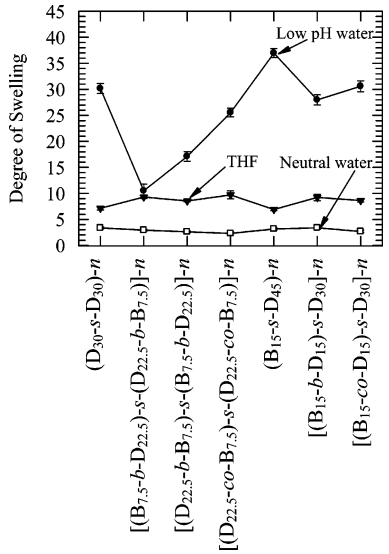

Figure 7. Degrees of swelling of the cross-linked star networks in low pH water, in neutral pH water, and in THF. D, B, *s*, and *n* are (further) abbreviations for DMAEMA, BzMA, *star*, and *network*, respectively.

the networks. In particular, as the pH was decreased, the DSs of all networks increased. This was due to the fact that all the networks contained DMAEMA ionizable units. DMAEMA is a weakly basic tertiary amine, which is uncharged at high pH but becomes positively charged at low pH.[40−43] The electrostatic repulsion created by the network charges and the osmotic pressure due to the chloride counterions at low pH both promoted network swelling. The importance of the DMAEMA charge was also confirmed by the fact that each DS versus pH curve followed closely the corresponding DI versus pH curve, discussed in the following section. Notable was the fact that all the networks started to swell at approximately the same value of pH, just below 6, with the exception of the DMAEMA homopolymer-based network, which started to swell below pH 7. This was in agreement with earlier studies, according to which the pH values below which the networks started to swell depended on their composition but were independent of the copolymer architecture.[30] In particular, higher p*K*'s were obtained for less hydrophobic amine-containing hydrogels.

Aqueous DSs at Low and Neutral pH and in THF. Figure 7 shows the aqueous DSs at low pH (at the DS maximum where pH = 3−5), the DSs at neutral pH, as well as the DSs in THF of all the networks. The DSs at low pH were higher than those in neutral water due to the ionization of the DMAEMA units at low pH. The DSs in THF were higher than the ones in neutral water because THF was a nonselective (good) solvent for the two types of monomer repeat units, DMAEMA and BzMA, while water is compatible only with the DMAEMA units.

The acidic DSs in Figure 7 seem to be determined by the length and composition of the elastic chains. ($BzMA_{15}$-*star*-$DMAEMA_{45}$)-*network* (network 5) presented the highest DS at low pH of around 37, due to the constitution of the network elastic chains from DMAEMA homopolymers with a high degree of polymerization (DP = 45). The DMAEMA homopolymer network and the two cross-linked heteroarm star-based networks, [($BzMA_{15}$-*b*-$DMAEMA_{15}$)-*star*-$DMAEMA_{30}$]-*network* and [($BzMA_{15}$-*co*-$DMAEMA_{15}$)-*star*-$DMAEMA_{30}$]-*network*, presented the second highest DSs, since their elastic chains also comprised DMAEMA homopolymer chains, but of lower DP than that of ($BzMA_{15}$-*star*-$DMAEMA_{15}$)-*network*. The three networks with amphiphilic copolymer elastic chains, [($BzMA_{7.5}$-*b*-$DMAEMA_{22.5}$)-*star*-($DMAEMA_{22.5}$-*b*-$BzMA_{7.5}$)]-*network*, [($DMAEMA_{22.5}$-*b*-$BzMA_{7.5}$)-*star*-($BzMA_{7.5}$-*b*-$DMAEMA_{22.5}$)]-*network*, and [($DMAEMA_{22.5}$-*co*-$BzMA_{7.5}$)-*star*-($DMAEMA_{22.5}$-*co*-$BzMA_{7.5}$)]-*network* (networks 2, 3, and 4, respectively), presented the lowest DSs due to the lower DMAEMA content of the elastic chains. [($DMAEMA_{22.5}$-*co*-$BzMA_{7.5}$)-*star*-($DMAEMA_{22.5}$-*co*-$BzMA_{7.5}$)]-*network*, network 4, did not present as low a DS as the other two networks, networks 2 and 3, due to the random distribution of the two monomers in the elastic chains. The random distribution of the BzMA units in the network allowed the unhindered expansion of the elastic and dangling chains of the network. The star block based networks, [($BzMA_{7.5}$-*b*-$DMAEMA_{22.5}$)-*star*-($DMAEMA_{22.5}$-*b*-$BzMA_{7.5}$)]-*network* and [($DMAEMA_{22.5}$-*b*-$BzMA_{7.5}$)-*star*-($BzMA_{7.5}$-*b*-$DMAEMA_{22.5}$)]-*network*, presented the lowest DSs because of microphase separation, since the hydrophobic blocks aggregate to form hydrophobic microdomains, as observed before for amphiphilic networks.[26]

The DSs of the amphiphilic conetworks in neutral water remained approximately constant, spanning a range of relatively low values, from 2.0 to 2.9. In contrast, network 1, the DMAEMA homopolymer-based network, presented a slightly higher DS in neutral water, equal to 3.4, due to the absence of the BzMA hydrophobic monomer and its more hydrophilic character compared to that of the amphiphilic conetworks. The DSs at neutral pH of the amphiphilic conetworks synthesized in this study were comparable to those of other amphiphilic star conetworks[30] as well as of amphiphilic conetworks based on linear triblock copolymers.[26]

The DSs of all networks in THF were higher than in neutral pH. In particular, the DSs in THF ranged from 6.9 to 9.7. This was attributed to the fact that both the BzMA and the DMAEMA units were more compatible with THF than with neutral water. THF was a nonselective solvent for these two monomer units, while neutral water was a selective solvent for the DMAEMA units, leading to a reduction in the swelling. The DMAEMA units were uncharged in both neutral water and THF. The similar DSs of all copolymer networks in THF suggested that the architecture did not affect the swelling of the networks in THF. Amphiphilic conetworks based on cross-linked DMAEMA−MMA star copolymers presented a higher range of DSs in THF, from 9.3 to 11.6, due to the higher arm

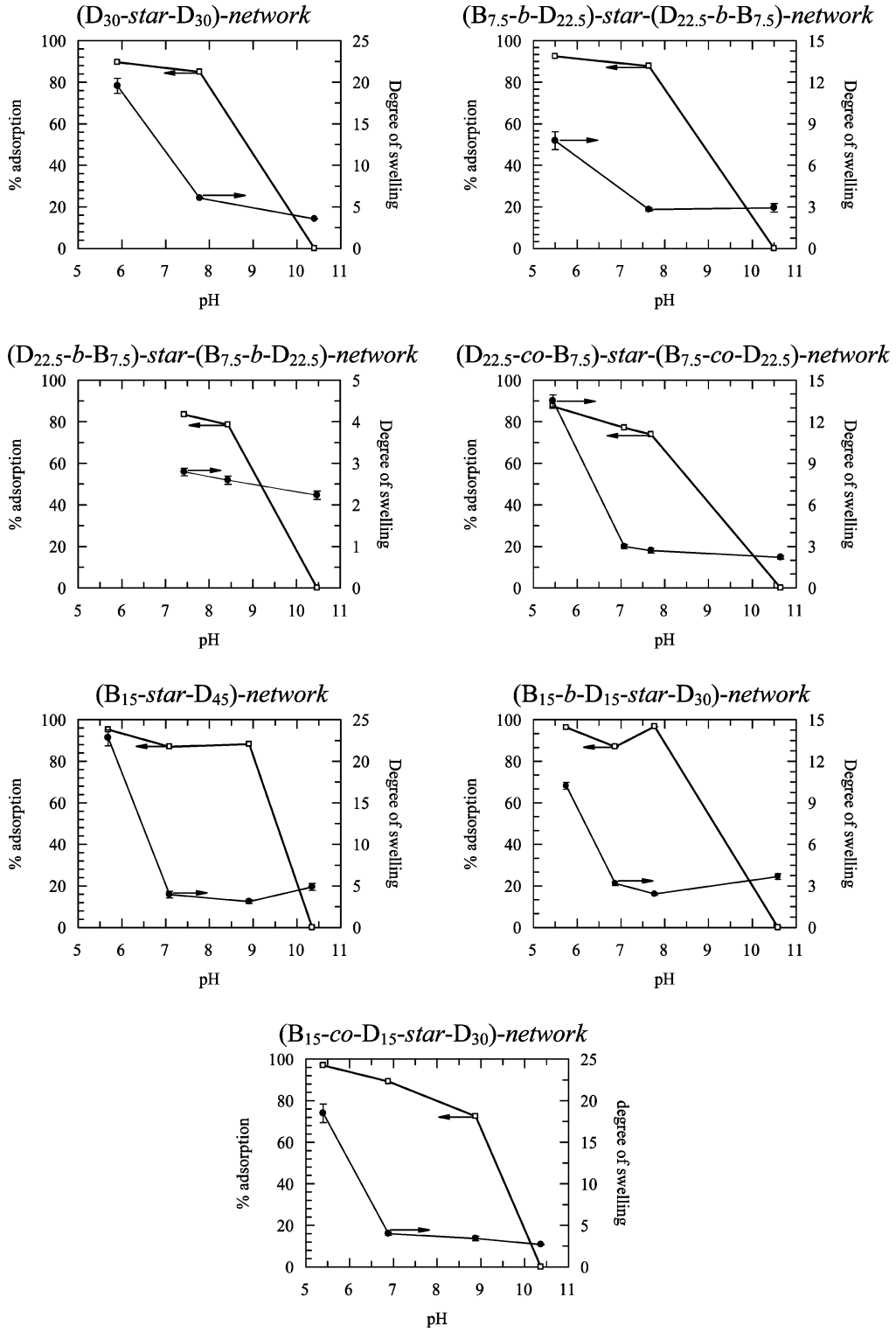

Figure 8. Percentage of adsorbed DNA onto and aqueous degrees of swelling of the cross-linked star networks as a function of pH.

DPs of 50 of the star polymers of that study compared to 30 of the star copolymers of the present study.

Effective pK's of the DMAEMA Units. Table 3 lists the effective p*K*'s of the DMAEMA units in the cross-linked star networks. The p*K*'s of the networks were read out from the DI versus pH curves as the pH at 50% ionization. All the networks were found to have similar p*K*'s, spanning a range of values from 4.8 to 5.5. The DMAEMA homopolymer network, network 1, presented the highest effective p*K* of 5.5, with the copolymer networks exhibiting p*K* values between 4.8 and 5.0. The lower effective p*K*'s of the amphiphilic copolymer networks were attributed to their greater hydrophobicity (due to the presence of BzMA), leading to the reduction of the dielectric constant, rendering ionization more difficult and reducing the p*K*. The p*K* values were not affected by the architecture of the networks as observed in other star-based amphiphilic conetworks (DMAEMA−MMA).[30] The range of the p*K* values was slightly lower than for DMAEMA−MMA star amphiphilic networks, with DP of the arm 50,[30] because of the greater hydrophobicity of the present system imparted by the presence of BzMA (more

hydrophobic than MMA) and by the greater content in the hydrophobic EGDMA cross-linker (higher cross-link density due to shorter arms).

DNA Adsorption Studies. This section presents the pH dependence of the adsorption of DNA onto the CLS-MACs. Figure 8 displays the percent DNA adsorption versus pH profiles for the seven networks. The DS versus pH profiles of the seven networks, measured in the presence of adsorbed DNA, are plotted on the second (right) *y*-axis of each graph. These DSs were close to, but systematically lower than, those in Figure 6 probably due to the presence of the adsorbed DNA.

The data in Figure 8 suggested that the DNA adsorption was driven by the electrostatic attractions between the negatively charged DNA (because of its phosphate groups) and the positively charged networks (due to the presence of the DMAEMA units) for pH below ~8. This is supported by the fact that there was no DNA adsorption for all seven networks at alkaline pH (pH > 10), where the DMAEMA units were uncharged, and also by the fact that adsorption was almost complete at pH 5.5, where the DMAEMA units were fully charged. This implies that DNA can be loaded onto the networks at low pH and delivered simply by adjusting the pH to a higher value.

DNA adsorption was high even when the DMAEMA units were slightly charged (pH 7−9). This was due to the fact that the ratio of the DMAEMA positive charges to the DNA negative charges was much higher than 1, since the concentration of the DNA solution added to the networks was low. Thus, even though the networks were only partially protonated at pH ~ 8, the positive charges of the DMAEMA units were sufficient to promote the adsorption of all DNA.

It is noteworthy that all seven networks presented similar DNA adsorption, independent of their structure. Even the DMAEMA homopolymer-based network, that was expected to exhibit higher adsorption, presented a similar adsorption. This also concludes that the DNA adsorption motif on these amphiphilic conetworks is electrostatic, as has been observed before for negatively charged proteins on DMAEMA−HEGMA networks.[28] Similar behavior has also been observed for proteins on methacrylic acid/acrylic acid microgels as well as for multivalent metal cations on sodium acrylate gels.[44,45]

Conclusions

The successful GTP synthesis of networks based on amphiphilic cross-linked "in−out" star polymers of various structures (heteroarm, block, and statistical stars) was accomplished using a monofunctional initiator in a four-, five-, or six-step preparation. It is noteworthy that GTP was active even after six monomer additions, allowing the synthesis of networks with such complicated structures. The degree of swelling of all the networks synthesized was measured in THF, in acidic, in neutral, and in alkaline water. In acidic water, the DSs were highest and depended on the network architecture. Almost complete adsorption of DNA onto all networks was measured even for low DIs of the DMAEMA units.

Acknowledgment. The University of Cyprus Research Committee (Grant 2000−2003) is thanked for financial support for this work. The A. G. Leventis Foundation is also thanked for a generous donation that enabled the purchase of the NMR spectrometer of the University of Cyprus.

References and Notes

(1) Patrickios, C. S.; Georgiou, T. K. *Curr. Opin. Colloid Interface Sci.* **2003**, *8*, 76−85.
(2) Erdodi, G.; Kennedy, J. P. *Prog. Polym. Sci.* **2006**, *31*, 1−18.
(3) Vamvakaki, M.; Patrickios, C. S. *J. Phys. Chem. B* **2001**, *105*, 4979−4986.
(4) Georgiou, T. K.; Vamvakaki, M.; Patrickios, C. S. *Polymer* **2004**, *45*, 7341−7355.
(5) Iván, B.; Kennedy, J. P.; Mackey, P. W. In *Polymeric Drugs and Drug Delivery Systems*; Dunn, R. L., Ottenbrite, R. M., Eds.; ACS Symposium Series 469; American Chemical Society: Washington, DC, 1991; pp 194−202.
(6) Iván, B.; Kennedy, J. P.; Mackey, P. W. In *Polymeric Drugs and Drug Delivery Systems*; Dunn, R. L., Ottenbrite, R. M., Eds.; ACS Symposium Series 469; American Chemical Society: Washington, DC, 1991; pp 203−212.
(7) Barakat, I.; Dubois, Ph.; Grandfils, Ch.; Jérôme, R. *J. Polym. Sci., Part A: Polym. Chem.* **1999**, *37*, 2401−2411.
(8) Zhu, C.; Hard, C.; Lin, C. P.; Gitsov, I. *J. Polym. Sci., Part A: Polym. Chem.* **2005**, *43*, 4017−4029.
(9) Scherble, J.; Thomann, R.; Iván, B.; Mülhaupt, R. *J. Polym. Sci., Part B: Polym. Phys.* **2001**, *39*, 1429−1436.
(10) Bruns, N.; Tiller, J. C. *Nano Lett.* **2005**, *5*, 45−48.
(11) Rimmer, S.; German, M. J.; Maughan, J.; Sun, Y.; Fullwood, N.; Ebdon, J.; MacNeil, S. *Biomaterials* **2005**, *26*, 2219−2230.
(12) Behravesh, E.; Jo, S.; Zygourakis, K.; Mikos, A. G. *Biomacromolecules* **2002**, *3*, 374−381.
(13) Alexandre, E.; Schmitt, B.; Boudjema, K.; Merrill, E. W.; Lutz, P. J *Macromol. Biosci.* **2004**, *4*, 639−648.
(14) Nicolson, P. C.; Vogt, J. *Biomaterials* **2001**, *22*, 3273−3283.
(15) Erdodi, G.; Kennedy, J. P. *J. Polym. Sci., Part A: Polym. Chem.* **2005**, *43*, 4965−4971.
(16) Erdodi, G.; Kennedy, J. P. *J. Polym. Sci., Part A: Polym. Chem.* **2005**, *43*, 3491−3501.
(17) Hild, G. *Prog. Polym. Sci.* **1998**, *23*, 1019−1149.
(18) Webster, O. W. *Science* **1991**, *251*, 887−893.
(19) Triftaridou, A. I.; Kafouris, D.; Vamvakaki, M.; Georgiou, T. K.; Krasia, T. C.; Themistou, E.; Hadjiantoniou, N.; Patrickios, C. S. *Polym. Bull.*, in press.
(20) Webster, O. W.; Hertler, W. R.; Sogah, D. Y.; Farnham, W. B.; RajanBabu, T. V. *J. Am. Chem. Soc.* **1983**, *105*, 5706−5708.
(21) Sogah, D. Y.; Hertler, W. R.; Webster, O. W.; Cohen, G. M. *Macromolecules* **1987**, *20*, 1473−1488.
(22) Dicker, I. B.; Cohen, G. M.; Farnham, W. B.; Hertler, W. R.; Laganis, E. D.; Sogah, D. Y. *Macromolecules* **1990**, *23*, 4034−4041.
(23) Webster, O. W. *J. Polym. Sci., Part A: Polym. Chem.* **2000**, *38*, 2855−2860.
(24) Webster, O. W. *Adv. Polym. Sci.* **2004**, *167*, 1−34.
(25) Simmons, M. R.; Yamasaki, E. N.; Patrickios, C. S. *Macromolecules* **2000**, *33*, 3176−3179.
(26) Triftaridou, A. I.; Hadjiyannakou, S. C.; Vamvakaki, M.; Patrickios, C. S. *Macromolecules* **2002**, *35*, 2506−2513.
(27) Demosthenous, E.; Hadjiyannakou, S. C.; Vamvakaki, M.; Patrickios, C. S. *Macromolecules* **2002**, *35*, 2252−2260.
(28) Loizou, E.; Triftaridou, A. I.; Georgiou, T. K.; Vamvakaki, M.; Patrickios, C. S. *Biomacromolecules* **2003**, *4*, 1150−1160.
(29) Vamvakaki, M.; Hadjiyannakou, S. C.; Loizidou, E.; Patrickios, C. S.; Armes, S. P.; Billingham, N. C. *Chem. Mater.* **2001**, *13*, 4738−4744.
(30) Vamvakaki, M.; Patrickios C. S. *Chem. Mater.* **2002**, *14*, 1630−1638.
(31) Georgiades, S. N.; Vamvakaki, M.; Patrickios, C. S. *Macromolecules* **2002**, *35*, 4903−4911.
(32) Georgiou, T. K.; Patrickios, C. S. *Macromolecules* **2006**, *39*, 1560−1568.
(33) Mykytiuk, J.; Armes, S. P.; Billingham, N. C. *Polym. Bull.* **1992**, *29*, 139−145.
(34) Rannard, S. P.; Billingham, N. C.; Armes, S. P.; Mykytiuk, J. *Eur. Polym. J.* **1993**, *29*, 407−414.
(35) Georgiou, T. K.; Vamvakaki, M.; Patrickios, C. S.; Yamasaki, E. N.; Phylactou, L. A. *Biomacromolecules* **2004**, *5*, 2221−2229.
(36) Georgiou, T. K.; Vamvakaki, M.; Phylactou, L. A.; Patrickios, C. S. *Biomacromolecules* **2005**, *6*, 2990−2997.
(37) Georgiou, T. K.; Phylactou, L. A.; Patrickios, C. S. *Biomacromolecules*, in press.
(38) Kanaoka, S.; Omura, T.; Sawamoto, M.; Higashimura, T. *Macromolecules* **1992**, *25*, 6407−6413.

(39) Tsitsilianis, C.; Voulgaris, D. *Macromol. Chem. Phys.* **1997**, *198*, 997−1007.
(40) Siegel, R. A.; Firestone, B. A. *Macromolecules* **1988**, *21*, 3254−3259.
(41) Siegel, R. A. *Adv. Polm. Sci.* **1993**, *109*, 233−267.
(42) Iván, B.; Feldthusen, J.; Müller, A. H. E. *Macromol. Symp.* **1996**, *102*, 81−90.
(43) Iván, B.; Haraszti, M.; Erdodi, G.; Scherble, J.; Thomann, R.; Mülhaupt, R. *Macromol. Symp.* **2005**, *227*, 265−274.
(44) Horkay, F.; Tasaki, I.; Basser, P. J. *Biomacromolecules* **2000**, *1*, 84−90.
(45) Horkay, F.; Tasaki, I.; Basser, P. J. *Biomacromolecules* **2001**, *2*, 195−199.

BM060699M